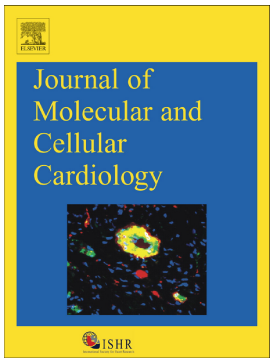

Localization of transcripts, translation, and degradation for spatiotemporal sarcomere maintenance

Yair E. Lewis, Anner Moskovitz, Michael Mutlak, Joerg Heineke, Lilac H. Caspi, Izhak Kehat

PII: S0022-2828(18)30021-X
DOI: doi:10.1016/j.yjmcc.2018.01.012
Reference: YJMCC 8671

To appear in: *Journal of Molecular and Cellular Cardiology*

Received date: 6 October 2017
Revised date: 14 January 2018
Accepted date: 19 January 2018

Please cite this article as: Yair E. Lewis, Anner Moskovitz, Michael Mutlak, Joerg Heineke, Lilac H. Caspi, Izhak Kehat , Localization of transcripts, translation, and degradation for spatiotemporal sarcomere maintenance. The address for the corresponding author was captured as affiliation for all authors. Please check if appropriate. Yjmcc(2018), doi:10.1016/j.yjmcc.2018.01.012

Localization of transcripts, translation, and degradation for spatiotemporal sarcomere maintenance

Yair E. Lewis[1], Anner Moskovitz[1], Michael Mutlak[1], Joerg Heineke[2], Lilac H. Caspi[1], Izhak Kehat*[1,3].

[1]The Rappaport Institute and the Bruce Rappaport Faculty of Medicine, Technion – Israel Institute of Technology, Haifa 31096, Israel.

[2]Experimental Cardiology, Klinik für Kardiologie und Angiologie, Medizinische Hochschule Hannover, Germany

[3]Department of Cardiology and the Clinical Research Institute at Rambam, Rambam Medical Center, Haifa 31096, Israel

Running title: Localization for sarcomere maintenance

*To whom correspondence should be addressed:
Izhak Kehat MD, PhD
The Rappaport Institute and the Bruce Rappaport Faculty of Medicine
Efron St. 6, POB 9649
Technion - Israel Institute of Technology,
Haifa 31096
Israel
Tel/fax: +972-4-8295378
ikehat@technion.ac.il

ABSTRACT

The mechanisms responsible for maintaining macromolecular protein complexes, with their proper localization and subunit stoichiometry, are incompletely understood. Here we studied the maintenance of the sarcomere, the basic contractile macromolecular complex of cardiomyocytes. We performed single-cell analysis of cardiomyocytes using imaging of mRNA and protein synthesis, and demonstrate that three distinct mechanisms are responsible for the maintenance of the sarcomere: mRNAs encoding for sarcomeric proteins are localized to the sarcomere, ribosomes are localized to the sarcomere with localized sarcomeric protein translation, and finally, a localized E3 ubiquitin ligase allow efficient degradation of excess unincorporated sarcomeric proteins. We show that these mechanisms are distinct, required, and work in unison, to ensure both spatial localization, and to overcome the large variability in transcription. Cardiomyocytes simultaneously maintain all their sarcomeres using localized translation and degradation processes where proteins are continuously and locally synthesized at high rates, and excess proteins are continuously degraded.

Keywords: Sarcomere; mRNA localization; localized synthesis; Ubiquitin proteasome

Abbreviations: NRVM, Neonatal rat ventricular cardiomyocytes; smFISH, Single Molecule Fluorescent In-Situ Hybridization; CV, Coefficient of variability; OPP, O-propargyl-puromcyin; AHA, L-azidohomoalaine; scRT–qPCR, single-cell quantitative polymerase chain reaction with reverse transcription; FPKM, Fragments Per Kilobase of transcript per Million mapped reads; mod-mRNAs, modified mRNAs; UTRs, untranslated regions; MuRF, muscle RING finger; TAC, transverse aortic constriction

1. INTRODUCTION

Macromolecular protein complexes play crucial roles in most cellular processes. Since the half-lives of proteins in these complexes is limited, long-living cells are required to continuously replace components or entire complexes. How these complex structures, with their distinct localization and proper subunit stoichiometry are maintained, is a key unanswered question in biology.

The cardiomyocyte is an excellent platform to study this question, since it is a specialized cell that is dedicated to operating and maintaining a heteromeric macromolecular protein complex, the sarcomere. In its core are the contractile myofilament proteins myosin and actin, and they are associated with other thick and thin filament, accessory, and regulatory proteins [1]. Sarcomeres are approximately 2.2 μm long, and are arranged serially in chains to form myofibrils that fill the cardiomyocyte cytoplasm. Each cell contains several hundred sarcomeres [2] (Supplemental Fig. 1A). While cardiomyocytes survive for many years [3], the half-lives of sarcomeric proteins are several days [4], therefore, sarcomeric proteins require continuous replacement.

The ability of cardiomyocytes to maintain their sarcomere stoichiometry is well established [5]. Previous studies showed that tagged overexpressed sarcomeric protein will incorporate to the sarcomere and replace the corresponding endogenous proteins, with degradation of excess ones [6,7]. This surplus protein degradation was presumed to be the mechanism solely responsible for sarcomere maintenance, however it does not explain how the cell can ensure the adequate delivery of protein subunits to all its sarcomeres. Interestingly, these studies also showed that a significant overexpression is needed for a near-complete replacement. For example, one such study evaluated several transgenic lines, and showed that a 5-fold overexpression level was required to replace an endogenous sarcomeric protein with a transgenic one [8], suggesting that as much as 80% of the expressed transgenic sarcomeric

proteins are rapidly degraded. With an energetic cost of 4 ATP molecules per peptide bond for synthesis, a mechanism that relies only on degradation of surpluses unincorporated nascent proteins for localization would be expected to be unsustainably inefficient, since most translated proteins would be degraded on their way from a distal translation site to the sarcomere.

Pioneering studies aimed at understating the mechanism of endogenous sarcomeric protein incorporation used neonatal cardiomyocytes and Myosin isotope in situ hybridization techniques, and suggested that Myosin mRNA distribution is intermyofibrillar and non-sarcomeric [9], and is dispersed through the cytoplasm of the cardiomyocytes [10]. These studies also showed that microtubules are necessary for the dispersal of *Myh6* mRNA outward from the nucleus, but suggested that myofibrillogenesis may occur independently of mRNA cytoplasmic dispersion and microtubule organization [11]. However, as the available techniques at the time lacked subcellular resolution, the precise dynamics or locations of transcription, translation, and degradation of endogenous sarcomeric proteins were not identified, and the mechanisms of sarcomere maintenance remain incompletely understood.

Transcription in mammalian cell lines, and more recently in the liver [12], was shown to have 'bursty' kinetics. This kinetic can generate variability in mRNA content, and could result in variable protein synthesis rates. Transcriptional variability may challenge the maintenance of strict stoichiometry, which is necessary for many heteromeric complexes such as the sarcomere. It is not known if such a variability exists in cardiomyocytes. Moreover, while mechanisms such as polyploidy, temporal averaging [12], and nuclear retention [13,14] can dampen some of the global mRNA level variability, cardiomyocytes also need to maintain stoichiometry locally, at each sarcomeric unit.

Here, we identify the challenges for sarcomere maintenance and show that three distinct mechanisms are responsible for the maintenance of the sarcomere: mRNAs encoding for the sarcomeric proteins are localized to the sarcomere, ribosomes are localized to the sarcomere

with localized sarcomeric protein translation, and finally, the ubiquitin proteasome system efficiently degrades excess unincorporated sarcomeric protein with a localized E3 ubiquitin ligase. Sarcomeric complexes are maintained by continuously active localized protein translation and degradation processes. We show that each of these mechanisms is indispensable, and all work in unison, to ensure robust and efficient spatial and stoichiometric control over sarcomere maintenance.

2. MATERIAL AND METHODS

2.1 Neonatal Rat Ventricular Myocytes (NRVM) isolation and culture

All animal experiments were performed in compliance with relevant laws and institutional guidelines, and approved by the local animal ethics committees of the Technion, Israel Institute of Technology. Neonatal rat ventricular cardiomyocytes (NRVM) were isolated using the neonatal cardiomyocyte isolation system (Worthington Biochemical Corporation) from 1-3 day old Wistar rat pups, according to the manufacturer's instructions. Cardiomyocyte fraction was purified by centrifugation in Percoll gradient. Cells were plated on 18mm glass coverslips or 35mm glass-bottom culture dishes which were coated in advance with Cultrex Basement Membrane Extract (BME; Trevigen) and cultured in DMEM/F-12 growth medium, with 15% fetal calf serum. Cytochalasin D (10µM, Sigma C8273), latrunculin A (0.5µg/ml, Cayman Chemical 10010630) and colcemid (50µg/ml, Sigma D7385) were used for disruption of cytoskeletal transport. Actinomycin-D (5µg/ml, Sigma) was used for transcription inhibition. MG-132 (10µmol/L, Sigma M7449), Bortezomib (10µM, Selleck Chemicals), and PYR-41 (5µM, Sigma N2915) were used for inhibition of proteasome mediated protein degradation.

2.2 Adult rat cardiomyocyte isolation

Adult rat cardiac myocytes were isolated and cultured as previously described by Michele and colleagues [7]. Briefly, adult Wistar rats were deeply anesthetized with ketamine and xylazine, and the hearts were removed and placed on ice in Krebs-Henseleit buffer containing 1 mM Ca^{2+} (KHB- Ca^{2+}). The aorta was cannulated, and hearts were attached to perfusion apparatus and perfused retrogradely for 5 min with KHB (Ca^{2+} free). Next, the heart was perfused for 15 minutes with enzyme solution containing Collagenase Type II (162 U/ml; Worthington) in KHB. $CaCl_2$ was gradually added to a final concentration of 0.75 mM and perfusion continued for 15 min. Heart was then removed from perfusion apparatus and minced in KHB- Ca^{2+} enzyme solution. The tissue was digested twice for 5 min with gentle trituration and isolated myocytes were pelleted by centrifugation. The myocytes were resuspended in 2% BSA, 1mM $CaCl_2$-KHB, and the solution was titrated to 1.75 mM Ca^{2+} with three additions of $CaCl_2$ over 15 min. The resulting myocytes were collected by centrifugation and resuspended in DMEM with 5% fetal calf serum. For smFISH and immunofluorescence imaging, freshly isolated adult cardiomyocytes were fixed in suspension with 3.5% formaldehyde for 15 minutes, and then washed with PBS. Cells were plated onto glass coverslips that were coated with Cell-Tak (Corning). This allowed for studying adult cardiac myocytes in their native state, as opposed to isolation protocols in which cells are plated and processed after 24-48 hours of culture. For the study of dedifferentiation, myocytes were cultured in serum free media. For cardiomyocyte single-cell RT-qPCR, following isolation cells were collected and processed as described below.

2.3 Cardiac Tissue Sections

Hearts were cut in half, flushed with cold PBS, and incubated for 3 hours in a solution of 3.5% formaldehyde in PBS. The heart was then incubated overnight at 4^{o}C in a cryoprotective solution consisting of 30% sucrose, 3.5% formaldehyde, in PBS. The following day the hearts were removed from cryoprotective solution, flushed with cold PBS, and snap frozen in 2-

methylbutane immersed in liquid nitrogen. Cardiac tissue was sectioned using a cryostat (Leica), and mounted on silane-coated glass slides or PLL-coated glass coverslips. Tissue sections were then processed for smFISH, immunofluorescence or click reaction.

2.4 RNA Single Molecule Fluorescence In-Situ Hybridization (smFISH)

We designed a library of 18-22 nucleotide long oligonucleotide probes for each gene using the probe designer tool freely available online (https://www.biosearchtech.com/stellarisdesigner/). Complete probe libraries are listed in Table S1. Each probe library contains between 20-50 short oligonucleotide probes that hybridize to the mRNA of interest and permit for visualization of mRNA at single molecule resolution. Probes were tagged with 5-TAMRA or Quasar-670 fluorophores. Probe libraries were purchased from Biosearch Technologies. For polyA FISH, we used 30 nucleotidet long polyT oligos each tagged with Alexa Fluor 647 (Integrated DNA Technologies). Hybridization proceeded as follows – 24 hours after isolation and culture as described above, cells or sections were washed with PBS, then fixed with a solution containing methanol:acetic acid (3:1) or 3.5% formaldehyde for 10 minutes. Prior to hybridization cells were washed with a buffer containing 10% formamide (deionized; Sigma). Hybridization was performed in a buffer containing 10% formamide, 10% dextran sulfate, 2X SSC and desired probe at a concentration of 125 nM. Hybridization was done overnight in a humidified chamber at 37°C, or 30°C for tissue sections. Following hybridization, cells were washed twice with 10% formamide wash buffer for 30 min. at 37°C or 30°C. Second wash was supplemented with 4′,6-diamidino-2-phenylindole dihydrochloride (DAPI) at a concentration of 1µg/ml for nuclear staining. Cells were then washed once with 2X SSC for 5 minutes and mounted on glass slides with 12 µl of Fluoromount-G (ThermoFisher Scientific), or with glucose oxidase – catalase anti-fade solution in case of Alexa-647 or Quasar-670 probe libraries [15].

2.5 smFISH Imaging and Analysis

Slides were imaged with Axio Observer inverted fluorescent microscope (Zeiss) using an X-cite metal-halide light source and a high-resolution camera (Hamamtsu Orca R2), with an X63/1.4NA objective (Olympus). Exposure times for smFISH signal was between 800-3000ms. Images were captured as a full thickness z-stack with a 0.24-0.30 µm section size. For qualitative analysis resulting images were imported into ImageJ, a Laplacian of Gaussian filter was applied to the smFISH channel using the LoG3D plugin [16], and a max intensity merge of the z-stack was acquired. Quantification of smFISH was performed using the FISH-quant MATLAB toolbox [17].

2.6 Immunofluorescence Staining

Immunofluorescence was performed on isolated cardiomyocytes (neonatal and adult rat) and heart frozen tissue sections. In the case of FISH experiments the immune-staining was done before FISH. In OPP experiments (see below), immunostaining followed the click reaction. Cells and tissue were permeabilized with 1% Triton or 70% ethanol, and blocked with a solution containing 5% bovine serum. Primary antibodies were incubated overnight at 4^{o}C. Primary antibodies used were against α-sarcomeric actinin, cardiac troponin I, ribosomal protein S6, Murf1, and DDDDK tag (FLAG). Secondary antibodies were incubated for 1 hour at room temperature. Nuclei were counterstained with DAPI for 10 minutes at room temperature. A full list of antibodies used can be found in Table S2.

2.7 Protein Synthesis Assay

For analyzing location of protein synthesis, we used the Click-iT Plus OPP Alexa Fluor 488 Protein Synthesis Assay Kit (ThermoFisher Scientific). Briefly, cardiomyocytes were incubated with O-propargyl-puromcyin (OPP). After specified time, 5-60 minutes depending on experiment, cells were fixed and permeabilized with 3% formaldehyde and 0.5% triton, and then a biorthogonal copper-catalyzed azide alkyne cycloaddition reaction (CuAAC, "click reaction") was performed between the alkyne containing OPP and the azide-conjugated fluorophore [18]. Nascent protein is observed as green signal. A similar protein synthesis assay was performed by incubating cells with the methionine analogue L-azidohomoalaine (AHA) followed by click reaction with alkyne-tagged Alexa Fluour-647. For *in-vivo* protein synthesis, adult C57/bl mice were anesthetized, and OPP was injected into the LV wall under echocardiographic guidance. Fluorescent Cy5 beads were injected along with the OPP for marking injection site. One hour following injection, the heart was excised, fixated and cryosectioned as described above. Click reaction was performed on the fixed tissue sections.

2.8 Protein Synthesis Image Analysis

For OPP images analysis we used the open source CellProfiler [19] software package. Sarcomeric α-actinin immunostaining was used to identify cardiomyocytes and their sarcomeres and measure the median α-actinin immunostaining intensity, and the median OPP fluorescence in areas that colocalize with the immunostaining (sarcomere) or outside it (background), for each cardiomyocyte. We also measured the total area of α-actinin immunostaining for each cell (sarcomeric area). The algorithm pipeline is available upon request.

2.9 Electron microscopy

Neonatal rat cardiomyocytes were isolated and cultured as described. For studying the effects of proteasome inhibition, cells were incubated with 10µmol/L MG-132 for 5h. A separate plate was cultured in regular cardiomyocyte medium as control. Cells were then fixed with cold 3.5%-glutaraldehyde in 0.1M sodium-cacodylate buffer. Specimens were post-fixated with 2% osmium-tetroxide and dehydrated using 50-100% ethyl-alcohol. For visualization, epon blocks were cut into thin-sections (70nm) and stained with 1% uranyl-acetate followed by 0.4% lead-citrate. Transmission electron microscopy was carried out using JEM 1011 (Jeol). Images were acquired and analyzed using Gatan Digital Micrograph (Gatan).

2.10 Single cell adult rat cardiomyocyte RT-qPCR

Cardiomyocytes were isolated from adult Wistar rats as described above. Immediately following isolation, cells were suspended in culture medium, and 2ml of the suspension was placed in a 10cm tissue culture plate. Sample was diluted as needed to allow for isolation of individual cardiomyocytes. Morphologically healthy-looking cardiomyocytes were identified, and single cells were collected one at a time into separate microtubes with a 100µm micropipette. RNA from each cell was isolated using the single-cell RNA purification kit (Norgen Biotek). cDNA from each cell was produced by reverse transcription using the iScript cDNA Synthesis kit (Bio-Rad). We then performed preamplification of the genes of interest with the SsoAdvanced PreAmp Supermix (Bio-Rad) with a primer pool containing primers (listed in Table S3). Following that, qPCR was done using a Bio-Rad CFX 96 thermocycler with the same primers used in the preamplification step. All studies were performed with a standard curve, technical duplicates, with negative, no reverse transcriptase, and positive (whole heart) controls.

2.11 Modified mRNA

Modified mRNAs were generated as previously described [20]. Two gene blocks of rat Tnni3 mRNA (*NM_017144.2)* tagged with FLAG epitope were designed and purchased from IDT (Table S4). One contained the full native Tnni3 mRNA including UTR's, while the other was designed with UTR's from pcDNA3.3_eGFP plasmid, a gift from Derrick Rossi (Addgene plasmid # 26822) [21]. Gene blocks also included T7 promoter. Modified mRNA was synthesized in-vitro using the MEGAscript T7 Transcription Kit (Invitrogen, AM1334). For control experiments we synthesized modified mRNA of GFP. Neonatal rat cardiomyocytes were transfected 48 hours after culture with the modified mRNA using the Stemfect RNA Transfection kit (Stemgent, 00-0069). The following day, cells were fixated and processed for immunofluorescence staining.

2.12 Generation of Troponin-FLAG fusion protein adenoviral vectors and viral transduction

Adenoviral vectors were constructed using the Gateway system (Invitrogen, Carlsbad, CA). The above mentioned Tnni3-FLAG gene blocks, with endogenous or synthetic UTR's, were cloned into the pENTR3c dual selection vector plasmid (Invitrogen) by using common restriction enzymes. The construct was combined with the adenoviral vector plasmid by performing the Gateway recombination LR reaction, creating a plasmid coding for adenovirus and the fusion mRNA under the control of a CMV promoter. HEK293 packaging cell line was transfected with the plasmid and a crude viral lysate was produced. The viral particles were further amplified by repeated steps of infection of HEK293 cells and finally purified using cesium gradients. Cultured NRVM were transduced by incubating cells with appropriate amount of purified adenovirus for 4 hours, then replacing culture medium.

2.13 Concentric hypertrophy model in mice using transverse aortic constriction

Pressure overload was performed as previously described [22].

2.14 Statistics

Analysis was performed using R (R Core Team (2016). R: A language and environment for statistical computing. R Foundation for Statistical Computing, Vienna, Austria. URL https://www.R-project.org/ with the Hmisc package (Frank E Harrell Jr, with contributions from Charles Dupont and many others. (2016). Hmisc: Harrell Miscellaneous. R package version 3.17-4. https://CRAN.R-project.org/package=Hmisc); the raster package (Robert J. Hijmans (2016). raster: Geographic Data Analysis and Modeling. R package version 2.5-8. https://CRAN.R-project.org/package=raster); corrplot package (Taiyun Wei and Viliam Simko (2016). corrplot: Visualization of a Correlation Matrix. R package version 0.77. https://CRAN.R-project.org/package=corrplot); gplot package (Gregory R. Warnes, Ben Bolker, Lodewijk Bonebakker, Robert Gentleman, Wolfgang Huber Andy Liaw, Thomas Lumley, Martin Maechler, Arni Magnusson, Steffen Moeller, Marc Schwartz and Bill Venables (2016). gplots: Various R Programming Tools for Plotting Data. R package version 3.0.1. https://CRAN.R-project.org/package=gplots).

3. RESULTS

3.1 Sarcomeric mRNA levels and ratios are variable in cardiomyocytes

To examine the spatial and temporal control of sarcomeric gene transcription we used single molecule mRNA fluorescence in situ hybridization (smFISH) [15]. This assay can identify both mature and nascent transcripts of endogenous genes [12]. Nascent mRNAs are located at the transcription sites, and visualized as high intensity nuclear spots, containing multiple transcripts. The number of nascent mRNAs can be calculated from the ratio of the intensities of the transcription site spots to the intensity of the cytoplasmic dots, representing single mRNAs [12]. The identity of the high intensity nuclear spots as active transcription sites was confirmed by

their disappearance with actinomycin D treatment (Supplemental Fig. 1B). We initially quantified the nascent and mature sarcomeric *Myh6, Myh7*, and *Actc1* transcripts in neonatal rat ventricular cardiomyocytes (NRVM), and observed a high variability in both the number of nascent mRNA at each transcription site, and the number of nascent mRNAs in each nucleus (Fig. 1A and B). This high variability is consistent with a stochastic bursty promoter behavior, which was also described for several metabolic liver genes [12]. Temporal averaging [12] and nuclear retention [13,14] were shown to dampen the variability resulting from busty transcription, but we nevertheless observed a high variability in the number of mature cytoplasmic mRNAs among cardiomyocytes (Fig. 1A and B). We next used dual color smFISH to study the ratio between the transcription of the two major sarcomeric genes *Myh6* and *Actc1*. There was a modest correlation between the number of nascent mRNAs of these two transcripts (Pearson's r=0.32), and the number of mature mRNAs (Pearson's r= 0.42), but the variability was high and the mature *Myh6*/*Actc1* mRNA ratio spanned more than two orders of magnitude in individual cardiomyocytes (Fig. 1C-F).

Next, we carefully examined adult cardiomyocytes in tissue sections. For quantitative dual color smFISH we analyzed only nuclei that were completely included in the section, and discarded nuclei in which neither *Myh6* nor *Actc1* nascent transcripts were observed, in order to exclude non-myocyte cardiac cells. The results in the homeostatic adult heart were very similar to those observed in NRVM, with high variability in the levels of each of the transcripts and a high variability in the ratio between them, among neighboring adult cardiomyocytes (Fig. 1G and H). Additionally, we noted variability between nascent *Myh6* transcription and the total transcription of the cardiomyocyte, and between the global level of transcripts, among neighboring cardiomyocytes (Supplemental Fig. 1C-E). We also analyzed *Actc1* transcripts using smFISH in isolated single adult cardiomyocytes (Fig. 1I). The results of this analysis are similar to the one

performed in neonatal cardiomyocytes, and show high variability. For technical reasons it was difficult to accurately count *Myh6* and *Myh7* transcripts in isolated adult cardiomyocytes.

For further quantification of mature mRNAs, we freshly isolated single adult cardiomyocytes, and performed single-cell quantitative PCR with reverse transcription (scRT–qPCR). In agreement with our smFISH data, this analysis demonstrated correlation but high variability in the levels of transcripts among adult cardiomyocytes (Fig. 1J-K and Supplemental Fig. 1F). Ratios between sarcomeric transcripts were variable between cardiomyocytes, and deviated from the expected protein product stoichiometry (Fig. 1L). Together these data show that both neonatal and adult cardiomyocytes are faced with variable levels of sarcomeric transcripts and transcript stoichiometry. This variability poses a major challenge for the maintenance of the sarcomere and its protein subunit stoichiometry.

3.2 Sarcomeric localization of mRNA in cardiomyocytes

Localization of mRNA was described in cells such as neurons but not in cardiac or skeletal muscle. Analysis of NRVM and adult rat heart sections showed that sarcomeric mRNAs (*Myh6, Myh7,* and *Actc1*) have a clear cross-striated sarcomeric localization in adult cardiomyocytes, with a less obvious sarcomeric distribution in NRVM (Fig. 2A, Supplemental Fig. 2A). The transcripts for the sarcoplasmic reticulum gene *Pln* did not display a prominent sarcomeric distribution in both neonatal and adult cardiomyocytes. The transcripts of *Dsp*, which encodes for the desmosome protein Desmoplakin showed a clear localization to the intercalated disc region in adult cardiomyocytes (Fig. 2A). A distinct sarcomeric cross-striated distribution of sarcomeric transcripts was also evident in freshly isolated adult cardiomyocytes (Fig. 2B). To measure the distribution of sarcomeric transcripts we employed a Fourier transform that demonstrated a power peak at the 2.2 µm cycle length, corresponding to the sarcomere length in these fixed heart tissues (Supplemental Fig. 2B). An analysis of adult mouse heart RNA-seq data expression data (GSE29278) [23], calculated as FPKM (Fragments Per Kilobase of

transcript per Million mapped reads), show that the sarcomeric genes are among the most highly expressed genes in the adult heart, and the 11 major sarcomeric genes out of 15,621 detectibly expressed genes (0.07%), are responsible for 12.7% of the transcriptome (Fig. 2C). We therefore studied the distribution of total mRNAs in both NRVM and in adult heart tissue with polyA FISH probes (Fig. 2D). This analysis shows that in both neonatal and adult cardiomyocytes most mRNA molecules in the cell have distinct cross-striated sarcomeric distribution, despite the less obvious localization pattern of individual transcripts in NRVM. This widespread distribution of sarcomeric localized mRNA throughout the cytoplasm ensures the abundance of sarcomeric transcripts at each sarcomeric complex.

3.3 Sarcomeric localization of protein translation in cardiomyocytes

Localization of mRNA enables, but does not guarantee, localized protein translation. We assessed the site of protein translation by using O-propargyl-puromycin (OPP). In this assay, nascent proteins were labelled by incubating NRVM with OPP, an aminoacyl-tRNA analog that efficiently incorporates into newly translated proteins [24], followed by fixation and fluorescent labeling (Supplemental Fig. 3A). This analysis showed intense localized protein translation throughout the cardiomyocytes in a clear sarcomeric pattern that colocalized with the Z-disc protein α-actinin (Fig. 3A and 3B and Supplemental Fig. 3B). Using the methionine analogue L-azidohomoalaine (AHA) to mark nascent proteins produced similar results (Fig. 3C).

To observe protein translation in vivo we injected OPP to the hearts of anesthetized mice, and harvested and fixed the tissue after 60 minutes (Fig. 3 D). This in vivo labeling of nascent proteins in the adult heart confirmed our observations in cultured cardiomyocytes, and shows that adult cardiomyocytes continuously and locally translate proteins at high rates at all their sarcomeres (Fig. 3E).

In addition to the location of protein synthesis, we examined the location of the translational machinery using immunostaining for RPS6, an evolutionary conserved essential part of the ribosome 40S subunit [25]. The distribution of RPS6 showed a sarcomeric pattern in NRVM (Fig. 3F), but the sarcomeric localization of ribosomes was much clearer in adult heart sections and isolated adult cardiomyocytes (Fig. 3G). We also observed variability in translation rates between cardiomyocytes (Supplemental Fig. 3C-G). Together these data show that high rate of localized protein translation occurs in all the sarcomeres throughout the cell, even in the quiescent heart.

Interestingly, we also noted intense localized translation at the junction between neighboring cardiomyocytes (Supplemental Fig. 3D and G). This area corresponds to the intercalated disc area, where we also noted localization of the desomosmal protein *Dsp* mRNA (Fig 2A). These observations suggest that similar to the sarcomere, localization of mRNA and localized protein translation also occurs in the intercalated disc.

3.4 Localization of mRNA and translation depends on cytoskeletal transport

We wanted to determine if the localized protein translation was responsible for anchoring and the localization of mRNA to the sarcomeres. We therefore inhibited translation using cycloheximide and examined mRNA localization with polyA FISH, and protein translation by using OPP. Cycloheximide completely blocked OPP incorporation, yet did not disrupt the sarcomeric localization of mRNAs in cardiomyocytes, showing that mRNA localization does not depend on translation (Fig. 4A). The active transport of mRNA along the cytoskeleton using motor complexes is the best-understood mechanism for mRNA translocation [26]. We next examined mRNA localization and protein translation using the actin polymerization inhibitors cytochalasin D and latrunculin A, or the microtubule-depolymerizing agent colcemid. Cells were incubated with the inhibitors for 3 hours to minimize secondary effects. This short-term inhibition of either actin or microtubule based transport partially disrupted the localization of mRNA and of

sarcomeric protein translation (Fig. 4B). These experiments show that active cytoskeletal transport is required for sarcomeric mRNA localization and the subsequent localized protein translation in cardiomyocytes.

3.5 Localized degradation of sarcomeric proteins

Several studies have elegantly shown that over-expression of sarcomeric genes, in viral vectors or as transgenes in vivo, resulted in appropriate incorporation of the encoded proteins to the sarcomere [7,8]. This incorporation was accompanied by stoichiometric replacement of the corresponding endogenous sarcomeric protein, with degradation of surplus unincorporated proteins.

To further explore the role of sarcomeric protein degradation in sarcomere maintenance we synthesized modified mRNAs (mod-mRNAs), allowing us to control the 5'-cap, the 5' and 3' untranslated regions (UTRs), the polyA tails of these mRNA [20], and directly transfect them to the cytoplasm, controlling the dose. These variables were shown to contribute to the localization of mRNA [26], and may be responsible for localized protein translation. We synthesized a rat *Tnni3-Flag* mod-mRNA with the endogenous *Tnni3* UTRs, and as controls used a GFP mod-mRNA with synthetic UTRs, or a *Tnni3-Flag* mod-mRNA in which we replaced the endogenous UTRs with the same synthetic UTRs used for the GFP (Fig. 5A). All three mod-mRNAs had the same 5'-cap and the same polyA tail. The transfection of the mod-mRNAs to NRVM resulted in precise localization of *Tnni3-Flag* protein to the sarcomere, in a pattern that was indistinguishable from the endogenous *Tnni3*, regardless of their UTRs. In, contrast GFP expression did not show a clear sarcomeric localization (Fig. 5B-D). Despite the transfection of large amounts of mod-mRNA for *Tnni3-Flag*, we did not observe an accumulation of excess *Tnni3* protein. These experiments agree with previous studies showing that even when highly overexpressed, transfected sarcomeric proteins, but not proteins like GFP, will incorporate to the sarcomere without excess accumulation.

Troponin-I has been reported to contain a nuclear localization signal and was observed in the nucleus in cardiac myocytes of adult humans [27]. Transfection of non-cardiac cells, led to nuclear accumulation of troponin-I (Supplemental Fig. 4A-B). We repeated the mod-mRNA transfection in the presence of the proteasome inhibitor MG-132 [28]. This treatment resulted in disruption of the sarcomeric structure with a significant nuclear accumulation of unincorporated troponin in cardiomyocytes (Fig. 5E), showing that troponin will accumulate if degradation is inhibited. Inhibition with an additional proteasome inhibitor Bortezomib, or the inhibition of ubiquitin-activating enzyme E1 with PYR-41 produced similar effects (Supplemental Fig. 4C-F). We also analyzed NRVM treated with MG-132 using electron microscopy and noted the disruption of the sarcomere structure with large accumulations of endogenous myofilaments in the cytoplasm (Fig. 5F), suggesting that endogenous sarcomeric proteins are normally translated in excess.

Efficient degradation of surplus unincorporated proteins can control protein quantities, but may also be a mechanism for controlling spatial localization. To further explore the independence of the localized translation from the protein degradation process, we inhibited the proteasome with MG-132 for 1 hour, and examined mRNA and protein synthesis localization (Fig 5G-H). Despite the inhibition of the proteasome we could still clearly observe precise sarcomeric localization of both mRNA and protein translation, albeit with some cytoplasmic accumulations of nascent proteins, conclusively showing that mRNA localization and localized protein translation are independent processes from the proteasome mediated degradation. We conclude that for endogenous sarcomeric proteins the ubiquitin-proteasome system serves to control protein quantities, is not required for localized protein translation, and these processes – localized sarcomeric protein translation, and efficient degradation of surplus proteins - continuously work in unison to maintain the sarcomere.

The proteasome system is highly efficient at removing excess sarcomeric proteins. MuRF1 (TRIM63), is an E3 ubiquitin ligase responsible for the degradation of sarcomeric proteins [29]. This protein shows a clear sarcomeric distribution in adult cardiomyocytes (Supplemental Fig. 5A-B).

3.6 Global analysis shows excessive sarcomeric gene transcription and translation

In a homeostatic tissue, a protein synthesis and degradation rates are equal. We matched transcripts expression levels (GSE29278) [23], with the degradation-time of 889 cardiac proteins, measured in vivo using metabolic $^{2}H_2O$ labeling in unstressed hearts [30] (Supplemental Fig. 5C). Unsupervised clustering segregated these proteins based on their mRNA levels and protein degradation-times. Surprisingly, functional enrichment analysis [31] of these clusters showed that this clustering also segregated the proteins to functional groups (Supplemental Fig. 5D). Specifically, the sarcomeric genes were clustered together as proteins with very high mRNA levels, relative to other abundant proteins with similar degradation times. Since mRNA levels correlate with protein translation rates, this analysis suggests that sarcomeric protein translation exceeds their degradation, yet such a mismatch is inconsistent with the steady state. A low translation rate of sarcomeric mRNAs, relative to other genes, could explain the discrepancy. To examine this option, we analyzed 'ribosome occupancy', a measure of translational efficiency. We matched the ribosome-bound mRNA levels in the heart [32] to the corresponding protein degradation time, and the results were similar (Supplemental Fig. 5E), demonstrating that sarcomeric genes are efficiently translated. Our mRNA transfection experiments suggest that sarcomeric proteins have two different half-lives; a longer one for proteins that were integrated to the sarcomere, and a very short one for unincorporated excess proteins, that could only be observed with proteasome inhibition. The earliest time point for analysis of protein degradation-time in the $^{2}H_2O$ dataset was one day [30], therefore the very short half-life of the unincorporated sarcomeric proteins was unmeasured, and explains the

apparent discrepancy between the high mRNA levels and rapid translation rate of sarcomeric proteins and their measured degradation time. Together these data indicate that in the homeostatic heart sarcomeric genes are translated in excess, with a very quick degradation of the surplus proteins. A proposed model for sarcomere maintenance is shown in Fig. 5I.

Finally, we examined the maintenance of the sarcomere in atrophy and hypertrophy. After isolation, adult cardiomyocytes have well organized sarcomeres. However, when cultured, the cells quickly round up at the edges, and exhibit a progressive decrease in the organization of their sarcomeres, and finally spread out [33]. Analysis of mRNA distribution shows that sarcomeric mRNAs lose their sarcomeric distribution and accumulate at the edges, where the cell rounding appears, within 24 hours (Supplemental Fig. 6A). After 5 days in culture, the cells no longer display localized protein translation at the edges, and the sarcomeres there appear disorganized (Supplemental Fig. 6B). Although the cause for the dedifferentiation is still not clear, and likely results from the lack of mechanical stimulation, these observations suggest that the loss of mRNA localization and the localized protein translation is associated with the dedifferentiation process.

In cardiac hypertrophy, cardiomyocytes grow by addition of sarcomeres [34,35]. We examined the expression of sarcomeric transcripts in mice, that have undergone a transverse aortic constriction (TAC) for 6 weeks. As expected, this pressure overload resulted in a significant 145% increase in the normalized heart weight of the animals ($p=0.0017$, $n=5$, Supplemental Fig. 7A). Gene expression analysis using RT-qPCR showed that the hypertrophy was associated with the well-established fetal gene expression program [36], with the upregulation of the skeletal actin isoform Acta1, and the myosin isoform *Myh7*, and with the downregulation of the myosin *Myh6* isoform (Supplemental Fig. 7B). Some other sarcomeric genes also showed a significant transcriptional increase, with an upregulation of Mybpc3, Tpm1, and Tnn2. In contrast, some transcripts showed a very modest and non-significant change (*Actc1, Tnnc1,*

Myom2, Myl2). These transcriptional changes however may not necessarily reflect the translation level of these genes. The ribosome-bound mRNA levels in the heart was studied in quiescence and 2 weeks after aortic banding [32]. This mRNA fraction may more accurately represent translated mRNAs [37]. Analysis of sarcomeric genes from this dataset indicates that most of the transcriptional changes observed after TAC do not alter the translation levels of these genes, and among the genes we analyzed only the 'translated-mRNA' levels of Nppb and Acta1 were significantly increased (Supplemental Fig. 7C). Such a mismatch between the mRNA and protein levela has been demonstrated for myosin in the human heart [38]. The proteomic study of protein degradation times in the heart also included an analysis in cardiac hypertrophy, induced by isoproterenol administered for 2 weeks [30]. For several sarcomeric genes we could match the ribosome-bound mRNA from the sham and TAC groups [32] to the degradation times of the proteins in control or isoproterenol groups [30] (Supplemental Fig. 7D). With the caveat of matching data from different hypertrophic stimuli (TAC and Isoproterenol), this analysis suggests that the degradation times of some, but not all sarcomeric proteins, may be prolonged during hypertrophy. Together these data support our model that sarcomeric proteins are synthesized in excess, with superfluous protein degradation even in the quiescent heart. Therefore, in cardiac hypertrophy, despite the large increase in sarcomeres and sarcomeric proteins, cardiomyocytes are not required to significantly increase the translation rate of these genes. Our analysis shows that there is localization of mRNAs and active proteins synthesis, which occurs simultaneously in all the sarcomeres of the cardiomyocyte, even in quiescence. Consequently, these tools cannot differentiate between existing and newly added sarcomeres, and cannot identify the location of these added sarcomeres.

4. DISCUSSION

In this study, we show that cardiomyocytes use multiple distinct mechanisms to exert both spatial and stoichiometric control over sarcomere maintenance. Sarcomeric genes are

transcribed in variable rates and ratios. To overcome this variability, and ensure the maintenance of all their sarcomeres, cardiomyocytes maintain large localized amounts of mRNA of sarcomeric genes. These high localized levels ensure the over-abundance of mRNA at all the cell's sarcomeres, and together with the localized ribosomes allow high rates of local sarcomeric protein synthesis. The localized proteasome degradation system rapidly degrades the excess unincorporated sarcomeric proteins, offsetting the transcriptional and translational variability. Our data also suggests that a similar process appears to occur at the intercalated discs.

We used smFISH to investigate transcriptional variability. While this approach is not without limitations, data from the scRT-qPCR shows similar results and patterns. We cannot determine if the cell-to-cell variability is intrinsic or extrinsic [13], but variable transcript ratios pose a major challenge for stochiometric sarcomere maintenance. The variability we show is similar in scale to the variability observed in liver genes [12].

The smFISH imaging of polyA mRNA suggests that most of the transcriptome has a cross striated sarcomeric localization in cardiomyocytes, but we also show localization of the desmosome gene *Dsp* transcript to the intercalated disc. Although mRNA localization was not shown before in cardiac or skeletal muscle, several mechanisms were proposed for mRNA localization in other cell types [39]. Some mRNA transcripts contain localization signals (called "zip codes") that are present in their 3' UTR, and responsible for their targeting to distinct locations. For example, the β-actin mRNA contains a 'zip code' in its 3' UTR, which is recognized by the RNA-binding protein zipcode-binding protein 1 (ZBP1) [40]. We did not notice a difference in the localization of troponin after transfection with a modified mRNA containing either the endogenous or synthetic UTRs, suggesting that a 3' UTR 'zipcode' is not a major mechanism for sarcomeric protein localization. Another mechanism that was proposed for mRNA localization is the translation dependent anchoring of mRNA, demonstrated for the ASH1 mRNA [41]. We show here that despite the complete inhibition of translation by cycloheximide,

sarcomeric transcripts were still highly localized. Therefore, localization of sarcomeric transcripts in cardiomyocytes does not depend on translation. We also show that active transport by the cytoskeleton is required for sarcomeric mRNA localization, with subsequent localized protein translation, but the specific molecules involved and the precise mechanisms of mRNA and ribosome localization in cardiomyocytes remains to be fully elucidated.

It is well known that cardiomyocytes regularly turn over their sarcomeric proteins, whose half-lives is limited to several days [42]. Such half-lives measurements showed, that despite being assembled in a 1:1:1 stoichiometry, troponin C has a much longer half-life than troponin I and T [43]. Therefore, in addition to the variability in expression we showed here, a replacement mechanism must also overcome a variation in protein half-lives between members of the sarcomeric complex. As noted, many studies have shown that overexpressed sarcomeric proteins can incorporate and stoichiometrically replace the endogenous sarcomeric proteins [5]. The adenoviral overexpression of troponin in cultured adult cardiomyocytes resulted in a progressive stoichiometric replacement of the endogenous protein, with no accumulation of excess transgene in the cytosol [7]. This study also showed that troponin I incorporated with even distribution between Z lines, while overexpressed tropomyosin showed initial pattern of incorporation at the M-line with progression toward the Z-lines with time. Together these studies demonstrated that replacement of sarcomeric protein is insensitive to the amount of mRNA, as long as the mRNA is in excess, and suggested that degradation could play a role in the replacement process.

The ubiquitin proteasome system was indeed reported to play a role in the turnover of proteins in the heart [44]. The muscle RING finger (MuRF) family of E3 ubiquitin ligases were shown to associate with the sarcomere and to degrade sarcomeric proteins [45,46]. Mice lacking both MuRF1 and MuRF2 developed hypertrophic cardiomyopathy with reduced ventricular function [47]. A similar phenotype was observe in mice lacking both MuRF1 and MuRF3 [48]. Efficient

degradation of surplus unincorporated proteins can offset the transcriptional, translational, and half-life imbalance and may also be used for spatial localization. However, on its own this mechanism cannot ensure the timely delivery of new sarcomeric proteins to each sarcomeric complex throughout the cytoplasm. Moreover, without localized protein translation, a highly active degradation system capable of destroying large quantities of nascent sarcomeric proteins, like the one present in cardiomyocytes, will likely degrade most translated proteins on their way from a distal translation site to the sarcomere.

We show here that cardiomyocytes employ three mechanisms for sarcomere maintenance - localization of mRNA, localization of ribosomes with localized protein translation, and the efficient degradation of unincorporated excess protein, and demonstrate that they are distinct, required, and work in unison. Localization of mRNA to sarcomeric complexes alone can contribute to, but cannot ensure the precise local translation we observed in all the sarcomeres, without localized ribosomes. Furthermore, mRNA localization cannot compensate for the imbalance in transcript levels and stoichiometry. Similarly, the localization of ribosomes alone can direct local translation, but cannot guarantee the availability of transcripts and thus the high translation rate we observed at each and every sarcomere in the cell, and cannot compensate for the transcriptional imbalance. We show that all these three processes are distinct and required by demonstrating that disruption of active cytoskeletal transport disrupts mRNA localization and the subsequent localized translation, that localization of mRNA occurs despite the inhibition of translation, and that without degradation excess sarcomeric proteins will accumulate, and the sarcomeric structure will be disrupted. Importantly, we show that precise localized mRNA and localized protein translation occur even when the proteasome is inhibited, conclusively demonstrating that these processes are independent, that degradation serves to correct quantity imbalance, and is not required for the spatial localization of endogenous sarcomeric proteins.

Although transcripts, ribosomes, and localized translation showed a sarcomeric pattern in neonatal cardiomyocytes, this pattern was not as precise as the sarcomeric pattern in adult cardiomyocytes, especially for the RPS6 staining. The less distinct sarcomeric pattern of ribosomes in the neonatal cells may stem from the lesser degree of sarcomere organization in these cells. It is also possible that neonatal cardiomyocytes rely more on mRNA localization than on ribosome localization, as compared to adult cells. We demonstrated that localization of mRNA, localization of ribosomes with localized protein translation, are distinct and required processes in neonatal cardiomyocytes, but due to technical limitations these experiments could not be performed in vivo. Since localization is even more precise in adult cardiomyocytes, it is likely that these conclusions also extend to adult cardiomyocytes in vivo.

Our global analysis, together with the OPP translation assay and the proteasome inhibition studies indicates that even quiescent cardiomyocytes actively synthesize endogenous sarcomeric proteins at excessively high rates in all their sarcomeres, with subsequent degradation of surplus unincorporated ones. Such a mechanism may enable the system to easily shift to hypertrophic growth. Our analysis of mRNA from mice after TAC and the analysis of ribosome-bound mRNA level after TAC [32], support this concept and indicate that hypertrophy is maintained with only a very modest increase in the translation rate of sarcomeric proteins. Older studies have also shown that while individual sarcomeric protein content increased progressively during cardiac hypertrophy of 1 month, the synthesis rate of these proteins was not increased [49,50].

The maintenance of protein complexes by a translation-degradation process has been proposed [51]. The spatial and temporal robustness offered by such a process however, does not come without a cost. Protein translation is energetically costly [52], and cardiomyocytes should invest considerable amount of energy to continuously transcribe, translate, and then rapidly degrade sarcomeric proteins. It is difficult to estimate the degree of this inefficiency, but it was shown that

15-30% of newly synthesized proteins in non-muscle cells are rapidly degraded [53]. As noted, the localization can increase the efficiency of the system by allowing translated proteins to immediately integrate to the nearby sarcomeres, possibly during their translation, and avoid degradation.

Taken together, these findings provide a comprehensive new understanding of protein complexes, such as the sarcomere, as very dynamic structures, which are maintained by a localized translation and degradation processes.

DISCLOUSRE

No conflict of interest to be disclosed.

ACKNOWLEDGMENTS

We thank the Biomedical Core Facility at the Faculty of Medicine, Technion, and the Pre - Clinical Research Authority at the Technion for their invaluable assistance. This study was supported in part by the Rappaport Family Institute for Research in the Medical Sciences, The Clinical Research Institute at Rambam, Rambam Medical Center, and The Israel Science Foundation [grants number 1424/16, 2243/17].

REFERENCES

[1] S. Sadayappan, The Myofilament Field Revisited in the Age of Cellular and Molecular Biology., Circ. Res. 121 (2017) 601–603. doi:10.1161/CIRCRESAHA.117.311629.

[2] A.J. Brady, Mechanical properties of isolated cardiac myocytes., Physiol. Rev. 71 (1991) 413–28. http://www.ncbi.nlm.nih.gov/pubmed/2006219 (accessed February 4, 2017).

[3] M.A. Laflamme, C.E. Murry, Heart regeneration., Nature. 473 (2011) 326–35. doi:10.1038/nature10147.

[4] A.F. Martin, Turnover of cardiac troponin subunits. Kinetic evidence for a precursor pool of troponin-I, J. Biol. Chem. 256 (1981) 964–968.

[5] B. Thompson, J. Metzger, Cell biology of sarcomeric protein engineering: disease modeling and therapeutic potential, Anat. Rec. 297 (2014) 1663–1669. http://onlinelibrary.wiley.com/doi/10.1002/ar.22966/full (accessed July 24, 2016).

[6] J. Robbins, Remodeling the Cardiac Sarcomere Using Transgenesis, Annu. Rev. Physiol. 62 (2000) 261–287. doi:10.1146/annurev.physiol.62.1.261.

[7] D.E. Michele, P.P. Albayya, J.M. Metzger, Thin filament protein dynamics in fully differentiated adult cardiac myocytes: Toward a model of sarcomere maintenance, J. Cell Biol. 145 (1999) 1483–1495. doi:10.1083/jcb.145.7.1483.

[8] S. Sadayappan, N. Finley, J.W. Howarth, H. Osinska, R. Klevitsky, J.N. Lorenz, P.R. Rosevear, J. Robbins, Role of the acidic N' region of cardiac troponin I in regulating myocardial function, FASEB J. 22 (2007) 1246–1257. doi:10.1096/fj.07-9458com.

[9] A.M. Ackermann, Z. Wang, J. Schug, A. Naji, K.H. Kaestner, Integration of ATAC-seq and RNA-seq identifies human alpha cell and beta cell signature genes., Mol. Metab. 5 (2016) 233–44. doi:10.1016/j.molmet.2016.01.002.

[10] G. Nikcevic, M. Perhonen, S.Y. Boateng, B. Russell, Translation is regulated via the 3' untranslated region of alpha-myosin heavy chain mRNA by calcium but not by its localization., J. Muscle Res. Cell Motil. 21 (2000) 599–607. http://www.ncbi.nlm.nih.gov/pubmed/11206137 (accessed October 6, 2017).

[11] M. Perhonen, W.W. Sharp, B. Russell, Microtubules are needed for dispersal of alpha-myosin heavy chain mRNA in rat neonatal cardiac myocytes., J. Mol. Cell. Cardiol. 30 (1998) 1713–22. doi:10.1006/jmcc.1998.0734.

[12] K. Halpern, S. Tanami, S. Landen, M. Chapal, L. Szlak, Bursty gene expression in the intact mammalian liver, Mol. Cell. 58 (2015) 147–56. http://www.sciencedirect.com/science/article/pii/S1097276515000507 (accessed July 19, 2016).

[13] N. Battich, T. Stoeger, L. Pelkmans, Control of Transcript Variability in Single Mammalian Cells, Cell. 163 (2015) 1596–1610. doi:10.1016/j.cell.2015.11.018.

[14] K. Bahar Halpern, I. Caspi, D. Lemze, M. Levy, S. Landen, E. Elinav, I. Ulitsky, S. Itzkovitz, Nuclear Retention of mRNA in Mammalian Tissues, Cell Rep. 13 (2015) 2653–2662. doi:10.1016/j.celrep.2015.11.036.

[15] A. Raj, P. van den Bogaard, S. a Rifkin, A. van Oudenaarden, S. Tyagi, Imaging individual mRNA molecules using multiple singly labeled probes, Nat. Methods. 5 (2008) 877–879. doi:10.1038/nmeth.1253.

[16] D. Sage, F.R. Neumann, F. Hediger, S.M. Gasser, M. Unser, Automatic tracking of individual fluorescence particles: Application to the study of chromosome dynamics, IEEE Trans. Image Process. 14 (2005) 1372–1383. doi:10.1109/TIP.2005.852787.

[17] F. Mueller, A. Senecal, K. Tantale, H. Marie-Nelly, N. Ly, O. Collin, E. Basyuk, E.

Bertrand, X. Darzacq, C. Zimmer, FISH-quant: automatic counting of transcripts in 3D FISH images, Nat. Methods. 10 (2013) 277–278. doi:10.1038/nmeth.2406.

[18] J. Liu, Y. Xu, D. Stoleru, A. Salic, Imaging protein synthesis in cells and tissues with an alkyne analog of puromycin, Proc. Natl. (2012). http://www.pnas.org/content/109/2/413.short (accessed July 24, 2016).

[19] A.E. Carpenter, T.R. Jones, M.R. Lamprecht, C. Clarke, I.H. Kang, O. Friman, D. a Guertin, J.H. Chang, R. a Lindquist, J. Moffat, P. Golland, D.M. Sabatini, CellProfiler: image analysis software for identifying and quantifying cell phenotypes., Genome Biol. 7 (2006) R100. doi:10.1186/gb-2006-7-10-r100.

[20] P.K. Mandal, D.J. Rossi, Reprogramming human fibroblasts to pluripotency using modified mRNA, Nat. Protoc. 8 (2013) 568–582. doi:10.1038/nprot.nprot.2013.019.

[21] L. Warren, P.D. Manos, T. Ahfeldt, Y.-H. Loh, H. Li, F. Lau, W. Ebina, P.K. Mandal, Z.D. Smith, A. Meissner, G.Q. Daley, A.S. Brack, J.J. Collins, C. Cowan, T.M. Schlaeger, D.J. Rossi, Highly Efficient Reprogramming to Pluripotency and Directed Differentiation of Human Cells with Synthetic Modified mRNA, Cell Stem Cell. 7 (2010) 618–630. doi:10.1016/j.stem.2010.08.012.

[22] I. Kehat, J. Davis, M. Tiburcy, F. Accornero, M.K. Saba-El-Leil, M. Maillet, A.J. York, J.N. Lorenz, W.H. Zimmermann, S. Meloche, J.D. Molkentin, Extracellular Signal-Regulated Kinases 1 and 2 Regulate the Balance Between Eccentric and Concentric Cardiac Growth, Circ. Res. 108 (2011) 176–183. doi:10.1161/CIRCRESAHA.110.231514.

[23] Y. Shen, F. Yue, D.F. McCleary, Z. Ye, L. Edsall, S. Kuan, U. Wagner, J. Dixon, L. Lee, V. V. Lobanenkov, B. Ren, A map of the cis-regulatory sequences in the mouse genome, Nature. 488 (2012) 116–120. doi:10.1038/nature11243.

[24] J. Liu, Y. Xu, D. Stoleru, A. Salic, Imaging protein synthesis in cells and tissues with an alkyne analog of puromycin., Proc. Natl. Acad. Sci. U. S. A. 109 (2012) 413–8. doi:10.1073/pnas.1111561108.

[25] O. Meyuhas, Ribosomal Protein S6 Phosphorylation, in: Int. Rev. Cell Mol. Biol., 2015: pp. 41–73. doi:10.1016/bs.ircmb.2015.07.006.

[26] M. Mofatteh, S.L. Bullock, SnapShot: Subcellular mRNA Localization., Cell. 169 (2017) 178–178.e1. doi:10.1016/j.cell.2017.03.004.

[27] O. Bergmann, R.D. Bhardwaj, S. Bernard, S. Zdunek, F. Barnabé-Heider, S. Walsh, J. Zupicich, K. Alkass, B.A. Buchholz, H. Druid, S. Jovinge, J. Frisén, Evidence for Cardiomyocyte Renewal in Humans, Science (80-.). 324 (2009) 98–102. http://science.sciencemag.org/content/324/5923/98 (accessed May 13, 2017).

[28] D.H. Lee, A.L. Goldberg, Proteasome inhibitors: valuable new tools for cell biologists, Trends Cell Biol. 8 (1998) 397–403. doi:10.1016/S0962-8924(98)01346-4.

[29] S. Perera, B. Mankoo, M. Gautel, Developmental regulation of MURF E3 ubiquitin ligases in skeletal muscle, J. Muscle Res. Cell Motil. 33 (2012) 107–122. doi:10.1007/s10974-012-9288-7.

[30] E. Lau, Q. Cao, D.C.M. Ng, B.J. Bleakley, T.U. Dincer, B.M. Bot, D. Wang, D.A. Liem, M.P.Y. Lam, J. Ge, P. Ping, A large dataset of protein dynamics in the mammalian heart proteome, Sci. Data. 3 (2016) 160015. doi:10.1038/sdata.2016.15.

[31] J. Chen, E.E. Bardes, B.J. Aronow, A.G. Jegga, ToppGene Suite for gene list enrichment analysis and candidate gene prioritization, Nucleic Acids Res. 37 (2009) W305–W311. doi:10.1093/nar/gkp427.

[32] P. Zhou, Y. Zhang, Q. Ma, F. Gu, D.S. Day, A. He, B. Zhou, J. Li, S.M. Stevens, D.

Romo, W.T. Pu, Interrogating translational efficiency and lineage-specific transcriptomes using ribosome affinity purification., Proc. Natl. Acad. Sci. U. S. A. 110 (2013) 15395–400. doi:10.1073/pnas.1304124110.

[33] R.L. Moses, W.C. Claycomb, Disorganization and reestablishment of cardiac muscle cell ultrastructure in cultured adult rat ventricular muscle cells, J. Ultrastruct. Res. 81 (1982) 358–374. doi:10.1016/S0022-5320(82)90064-8.

[34] B. Russell, M.W. Curtis, Y.E. Koshman, A.M. Samarel, Mechanical stress-induced sarcomere assembly for cardiac muscle growth in length and width., J. Mol. Cell. Cardiol. 48 (2010) 817–23. doi:10.1016/j.yjmcc.2010.02.016.

[35] S. Göktepe, O.J. Abilez, K.K. Parker, E. Kuhl, A multiscale model for eccentric and concentric cardiac growth through sarcomerogenesis, J. Theor. Biol. 265 (2010) 433–442. doi:10.1016/j.jtbi.2010.04.023.

[36] J. Machackova, J. Barta, N.S. Dhalla, Myofibrillar remodeling in cardiac hypertrophy, heart failure and cardiomyopathies., Can. J. Cardiol. 22 (2006) 953–68. http://www.ncbi.nlm.nih.gov/pubmed/16971981 (accessed January 9, 2018).

[37] M. Heiman, R. Kulicke, R.J. Fenster, P. Greengard, N. Heintz, Cell type–specific mRNA purification by translating ribosome affinity purification (TRAP), Nat. Protoc. 9 (2014) 1282–1291. doi:10.1038/nprot.2014.085.

[38] S. Miyata, W. Minobe, M.R. Bristow, L.A. Leinwand, Myosin heavy chain isoform expression in the failing and nonfailing human heart., Circ. Res. 86 (2000) 386–90. http://www.ncbi.nlm.nih.gov/pubmed/10700442 (accessed January 11, 2018).

[39] A.R. Buxbaum, G. Haimovich, R.H. Singer, In the right place at the right time: visualizing and understanding mRNA localization., Nat. Rev. Mol. Cell Biol. 16 (2015) 95–109.

doi:10.1038/nrm3918.

[40] V.L. Patel, S. Mitra, R. Harris, A.R. Buxbaum, T. Lionnet, M. Brenowitz, M. Girvin, M. Levy, S.C. Almo, R.H. Singer, J.A. Chao, Spatial arrangement of an RNA zipcode identifies mRNAs under post-transcriptional control, Genes Dev. 26 (2012) 43–53. doi:10.1101/gad.177428.111.

[41] I. Gonzalez, S.B. Buonomo, K. Nasmyth, U. von Ahsen, ASH1 mRNA localization in yeast involves multiple secondary structural elements and Ash1 protein translation., Curr. Biol. 9 (1999) 337–40. http://www.ncbi.nlm.nih.gov/pubmed/10209099 (accessed December 25, 2017).

[42] A.W. Everett, G. Prior, R. Zak, Equilibration of leucine between the plasma compartment and leucyl-tRNA in the heart, and turnover of cardiac myosin heavy chain., Biochem. J. 194 (1981) 365–8. http://www.ncbi.nlm.nih.gov/pubmed/6914197 (accessed December 25, 2017).

[43] A.F. Martin, Turnover of cardiac troponin subunits. Kinetic evidence for a precursor pool of troponin-I., J. Biol. Chem. 256 (1981) 964–8. http://www.ncbi.nlm.nih.gov/pubmed/7451483 (accessed December 25, 2017).

[44] A.L. Portbury, M.S. Willis, C. Patterson, Tearin' up my heart: proteolysis in the cardiac sarcomere., J. Biol. Chem. 286 (2011) 9929–34. doi:10.1074/jbc.R110.170571.

[45] J.A. Spencer, S. Eliazer, R.L. Ilaria, J.A. Richardson, E.N. Olson, Regulation of microtubule dynamics and myogenic differentiation by MURF, a striated muscle RING-finger protein., J. Cell Biol. 150 (2000) 771–84. doi:10.1083/JCB.150.4.771.

[46] T. Centner, J. Yano, E. Kimura, A.S. McElhinny, K. Pelin, C.C. Witt, M.-L. Bang, K. Trombitas, H. Granzier, C.C. Gregorio, H. Sorimachi, S. Labeit, Identification of muscle

specific ring finger proteins as potential regulators of the titin kinase domain, J. Mol. Biol. 306 (2001) 717–726. doi:10.1006/JMBI.2001.4448.

[47] C.C. Witt, S.H. Witt, S. Lerche, D. Labeit, W. Back, S. Labeit, Cooperative control of striated muscle mass and metabolism by MuRF1 and MuRF2., EMBO J. 27 (2008) 350–60. doi:10.1038/sj.emboj.7601952.

[48] J. Fielitz, M.-S. Kim, J.M. Shelton, S. Latif, J.A. Spencer, D.J. Glass, J.A. Richardson, R. Bassel-Duby, E.N. Olson, Myosin accumulation and striated muscle myopathy result from the loss of muscle RING finger 1 and 3., J. Clin. Invest. 117 (2007) 2486–95. doi:10.1172/JCI32827.

[49] N.M. Magid, J.S. Borer, M.S. Young, D.C. Wallerson, C. DeMonteiro, Suppression of protein degradation in progressive cardiac hypertrophy of chronic aortic regurgitation., Circulation. 87 (1993) 1249–57. doi:10.1161/01.CIR.87.4.1249.

[50] N.M. Magid, D.C. Wallerson, J.S. Borer, Myofibrillar protein turnover in cardiac hypertrophy due to aortic regurgitation., Cardiology. 82 (1993) 20–9. http://www.ncbi.nlm.nih.gov/pubmed/8519006 (accessed December 26, 2017).

[51] S.B. Cambridge, F. Gnad, C. Nguyen, J.L. Bermejo, M. Krüger, M. Mann, Systems-wide proteomic analysis in mammalian cells reveals conserved, functional protein turnover., J. Proteome Res. 10 (2011) 5275–84. doi:10.1021/pr101183k.

[52] N. Lane, W. Martin, The energetics of genome complexity, Nature. 467 (2010) 929–934. doi:10.1038/nature09486.

[53] F. Wang, L.A. Canadeo, J.M. Huibregtse, Ubiquitination of newly synthesized proteins at the ribosome, Biochimie. 114 (2015) 127–133. doi:10.1016/j.biochi.2015.02.006.

Figure Legends

Fig.1: Sarcomeric mRNA levels and ratios are variable in cardiomyocytes. (A) smFISH images of *Myh6* in NRVM display high variability in the amounts of nascent mRNA (arrowheads), and mature cytoplasmic mRNA, between neighboring cardiomyocytes, that have similar sarcomeric structure. *Myh6* smFISH signal (red), sarcomeric α-actinin immunostaining (green), DAPI (blue). (representative of 4 independent experiments). Scale bar, 10μm. (B) Probability density function (PDF) plots of the number of nascent mRNAs per transcription site (TS), and mature mRNA in the nucleus and cytoplasm in NRVM, demonstrating high variability. The coefficient of variation (CV) is shown below for each plot (n=47, 41, and 43 cardiomyocytes for *Myh6*, *Myh7*, and *Actc1* respectively). (C) Representative dual color smFISH images of *Actc1* (red) and *Myh6* (yellow) in NRVM showing high transcriptional variability. (D-E) Correlation plots of nascent (D) and mature (E) mRNA numbers in individual NRVM detected by dual color smFISH, showing modest correlation but high variability (Pearson's r=0.32, p=0.0035; r=0.42, p<0.0001 for nascent and mature mRNAs respectively, n=81). (F) Kernel density plot of the mature *Myh6*/*Actc1* mRNA ratio in individual cardiomyocytes that span more than two orders of magnitude (n=81). (G) Dual color smFISH images of *Actc1* (red) and *Myh6* (green) in adult heart tissue sections showing high variability. A nucleus with relatively high levels of both nascent *Actc1* and *Myh6* mRNAs (white arrows and arrowheads respectively), and a nucleus with low nascent *Actc1* but high nascent *Myh6* mRNAs levels (yellow arrowheads) are highlighted (representative of 2 independent experiments). Scale bar, 10μm. (H) Plot of nascent mRNA numbers detected by dual color smFISH in individual adult cardiomyocytes shows correlation, with high variability (Pearson's r =0.58, p=0.003 n=25 nuclei). (I) Probability density function (PDF) plots of the number of nascent mRNAs per transcription site (TS), and mature mRNA in the nucleus and cytoplasm in isolated adult cardiomyocytes, demonstrating high variability. The coefficient of variation (CV) is shown below the plot (n=32 cardiomyocytes). (J) Heatmap of single adult

cardiomyocytes RT-qPCR relative expression, demonstrating high variability (n=40). (K) Plot of the coefficient of variation (CV) for the expression of genes in the single adult cardiomyocytes. (L) Ratios between transcript pairs, derived from the single adult cardiomyocytes RT-qPCR. The known protein stoichiometry is shown as a dashed line.

Fig. 2. Sarcomeric localization of mRNA in cardiomyocytes. (A) smFISH images for the indicated genes in NRVM (top) and adult heart tissue sections (bottom). smFISH signal (white), DAPI (blue). Sarcomeres indicated by arrow (each image is representative of at least 3 independent experiments). (B) smFISH images of freshly isolated adult cardiomyocytes. Sarcomeres are indicated by arrows (each image is representative of at least 5 independent experiments). (C) Pie chart showing that 12.7% of the transcriptome is comprised of transcripts of 11 sarcomeric genes. (D) smFISH images of NRVM (left) and adult cardiac tissue sections (right) showing a clear sarcomeric distribution of the majority of transcripts in NRVM and in adult cardiomyocytes using polyA FISH probes (each image is representative of at least 3 independent experiments). Scale bar, 10µm; inset, 3µm for (A), (B) and (D).

Fig 3. Sarcomeric localization of protein translation in cardiomyocytes. (A) Imaging of newly synthesized proteins by pulse labeling NRVM with OPP for 30 min (green), shows that translation is highly localized to the sarcomere. Cells were co-immunostained with sarcomeric α-actinin antibodies (red), and DAPI (blue). Scale bar, 10µm; inset, 3µm (representative of 70 images, 7 independent experiments). (B) Line scan through cardiomyocyte image demonstrates co-localization of the OPP labeling (green) and sarcomeric actinin immunostain (red). (C) Imaging of newly synthesized proteins using AHA (red) shows that translation is highly localized to the sarcomere. DAPI (blue). Scale bar, 10 µm; inset, 3µm. (representative of 15 images, 3 independent experiments). (D) In vivo protein synthesis analysis was done by direct injection of OPP to the left ventricular wall, followed by harvesting and fixation after 60 minutes. (E) The in vivo imaging of newly synthesized proteins with OPP (green) shows high localized translation in

sarcomeres and at the intercalated discs (arrow). Fluorescent microbeads (red) mixed with the OPP mark the injection site. Scale bar, 10µm; inset, 3µm. (representative of 10 images, 3 independent experiments). (F) Imaging of ribosomes using RPS6 immunostaining (red) in NRVM shows sarcomeric localization. α-actinin immunostaining (green), DAPI (blue). Scale bar, 10 µm; inset, 3µm. (G) Immunostaining with RPS6 antibodies (red, left) shows sarcomeric distribution of ribosomes in adult cardiomyocytes in tissue sections. (representative of 10 images, 2 independent experiments). Scale bar, 50 µm; inset, 15µm. On the right, similar distribution in isolated adult cardiomyocytes. Scale bar, 10 µm; inset, 3µm.

Fig 4: Localization of mRNA transcripts and protein synthesis in cardiomyocytes involves active transport along the cytoskeleton. (A) polyA smFISH and OPP assay in NRVM after 3h incubation with cycloheximide. Control panels (left) demonstrate sarcomeric localization of both mRNA and protein synthesis. After treatment with cycloheximide (right) protein translation was inhibited, while sarcomeric localization of mRNA was unaffected. Scale bar, 10 µm; inset, 1.5µm. (B) smFISH and OPP in NRVM after disruption of the cytoskeleton by 3h incubation with cytochalasin D (10µM), latrunculin A (0.5µg/ml) or colcemid (50µg/ml). Control images show sarcomeric localization of mRNA transcripts and protein translation. After treatment with cytoskeletal inhibitors both polyA smFISH (white) and OPP (green) appear diffuse, with less pronounced sarcomeric distribution. OPP (green), polyA smFISH (white), DAPI (blue). Scale bar, 10 µm; inset, 1.5µm.

Fig 5. High rate of sarcomeric gene translation is offset by rapid degradation for dosage control. (A) Schematic representation of the modified mRNAs used. (B-D) Images of NRVM following transfection with GFP mod-mRNA showing diffuse distribution of GFP (green) in the cytoplasm and nucleus (B), while transfection with either the endogenous UTR (C), or the synthetic UTR (D) Tnni3-flag resulted in precise localization of Tnni3-flag to the sarcomere (Anti-flag, yellow). Anti-troponin I, identifying both the endogenous and transfected Tnni3 (red), DAPI (blue). Scale

bar, 10µm; inset, 3µm. (representative of 3 independent experiments). (E) Transfection with Tnni3-flag was performed as in (C) with MG-132, resulting in disruption of the sarcomeric structure and accumulation of large amounts of unincorporated Tnni3-flag in the nucleus. Scale bar, 10µm; inset, 3µm. (F) Electron microscopy images of NRVM showing large accumulations of disordered myofibrils (arrow) in the cytoplasm of MG-132 treated cardiomyocytes. Scale bar, 2 µm. (G) NRVM were incubated with MG-132 for 1 hour, and mRNA distribution was assessed by polyA smFISH (white). Despite the inhibition of proteasome mediated degradation, mRNAs still display a strong cross-striated sarcomeric pattern. Scale bar, 10µm; inset, 3µm. (H) NRVM were incubated with MG-132 for 1 hour, and the location of protein synthesis was assessed by OPP (green). Cells were also stained for troponin (red). (I) Proposed model of sarcomere maintenance: the transcription rate of sarcomeric genes is variable, and cardiomyocytes keep large, localized amounts of these mRNAs in all their sarcomeres. Cardiomyocytes locally translate these mRNAs, using sarcomeric localized ribosomes, at high rates at each sarcomere. The localized proteasome system rapidly degrades excess unincorporated sarcomeric proteins, offsetting the transcriptional and translational variability. The three mechanisms - localization of mRNA, localization of ribosomes, and the efficient degradation of unincorporated excess protein - all work in unison to ensure robust and efficient spatial and quantity control of sarcomeric proteins.

Figure 1

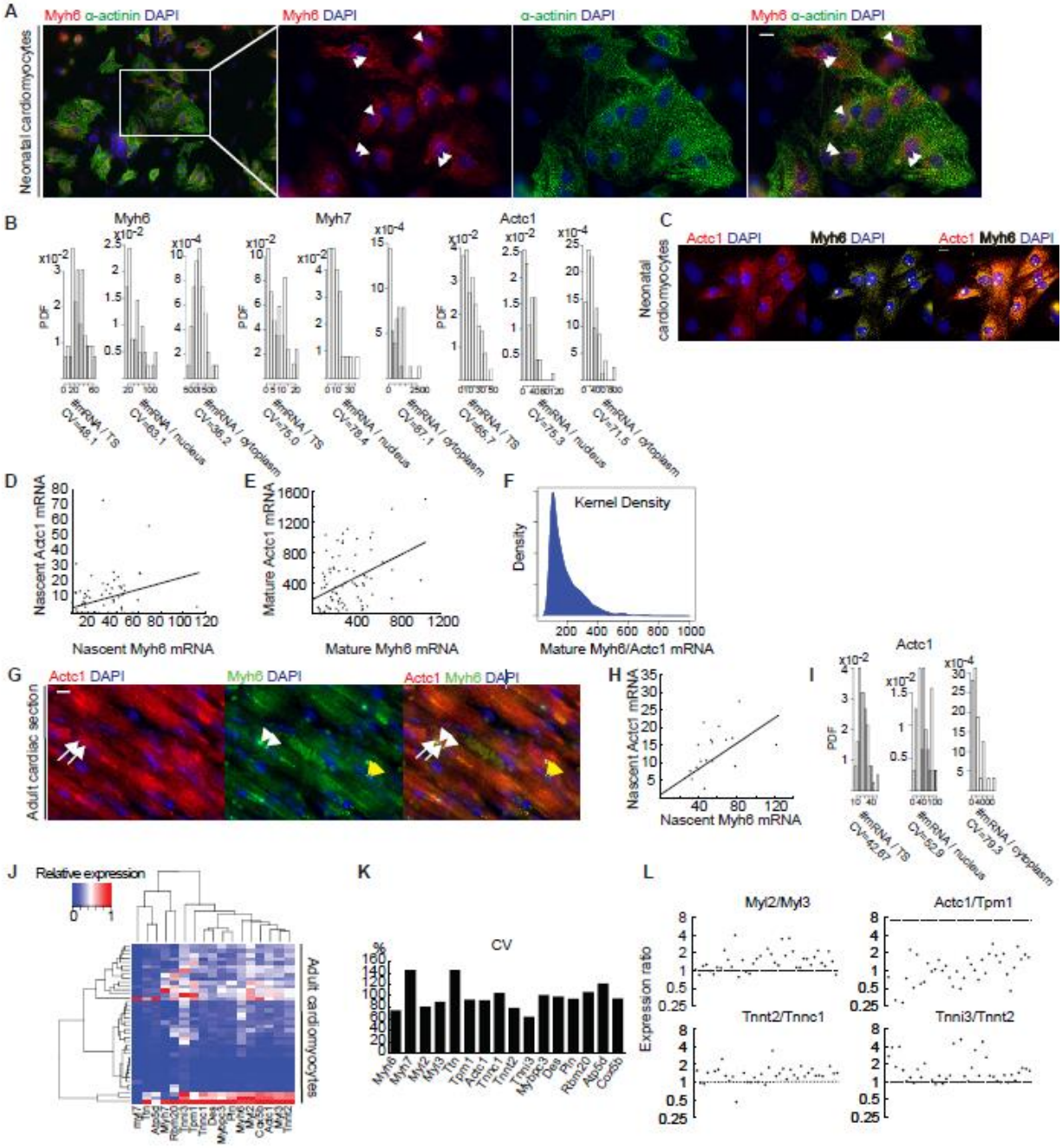

Figure 2

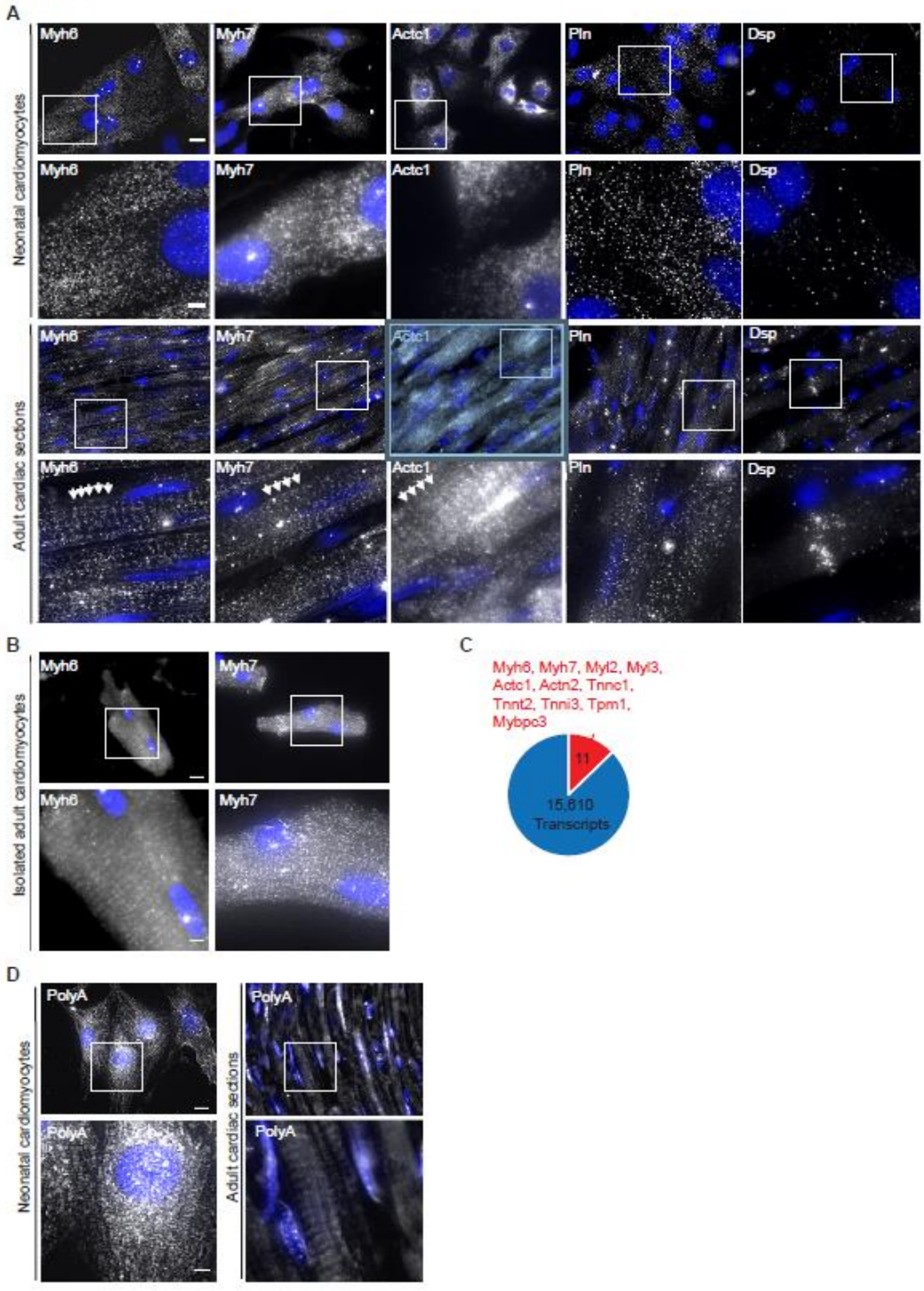

Figure 3

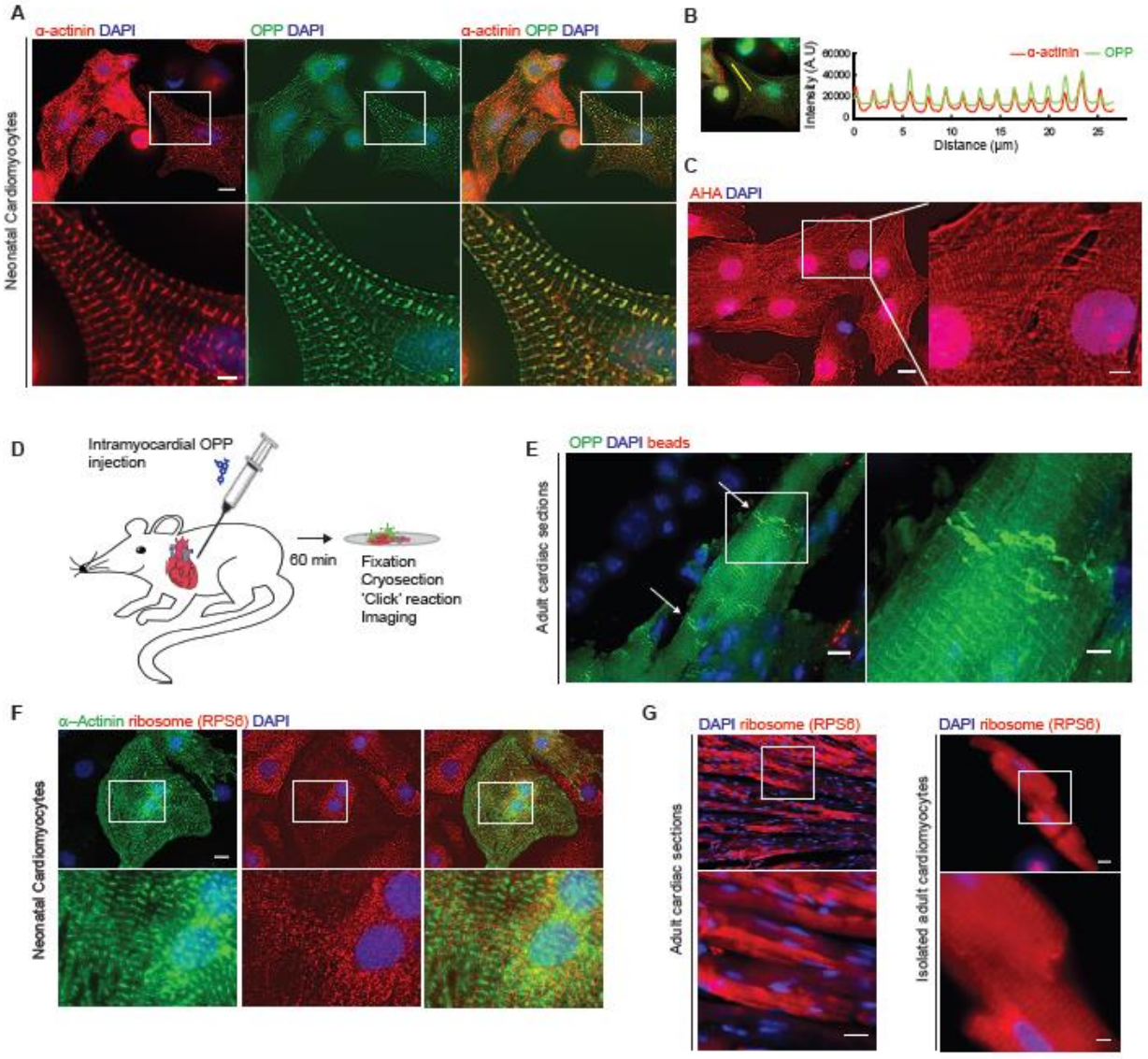

Figure 4

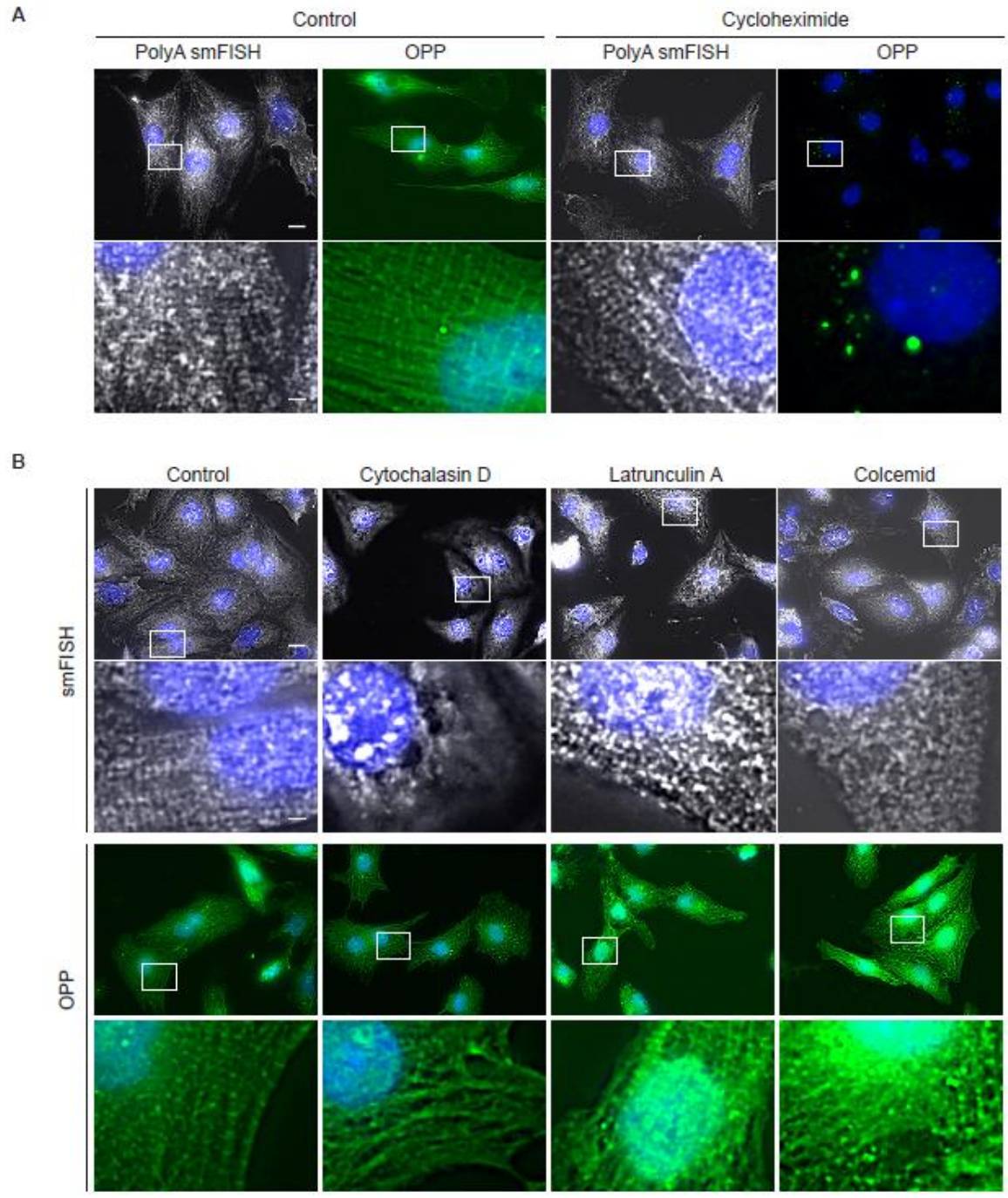

Figure 5

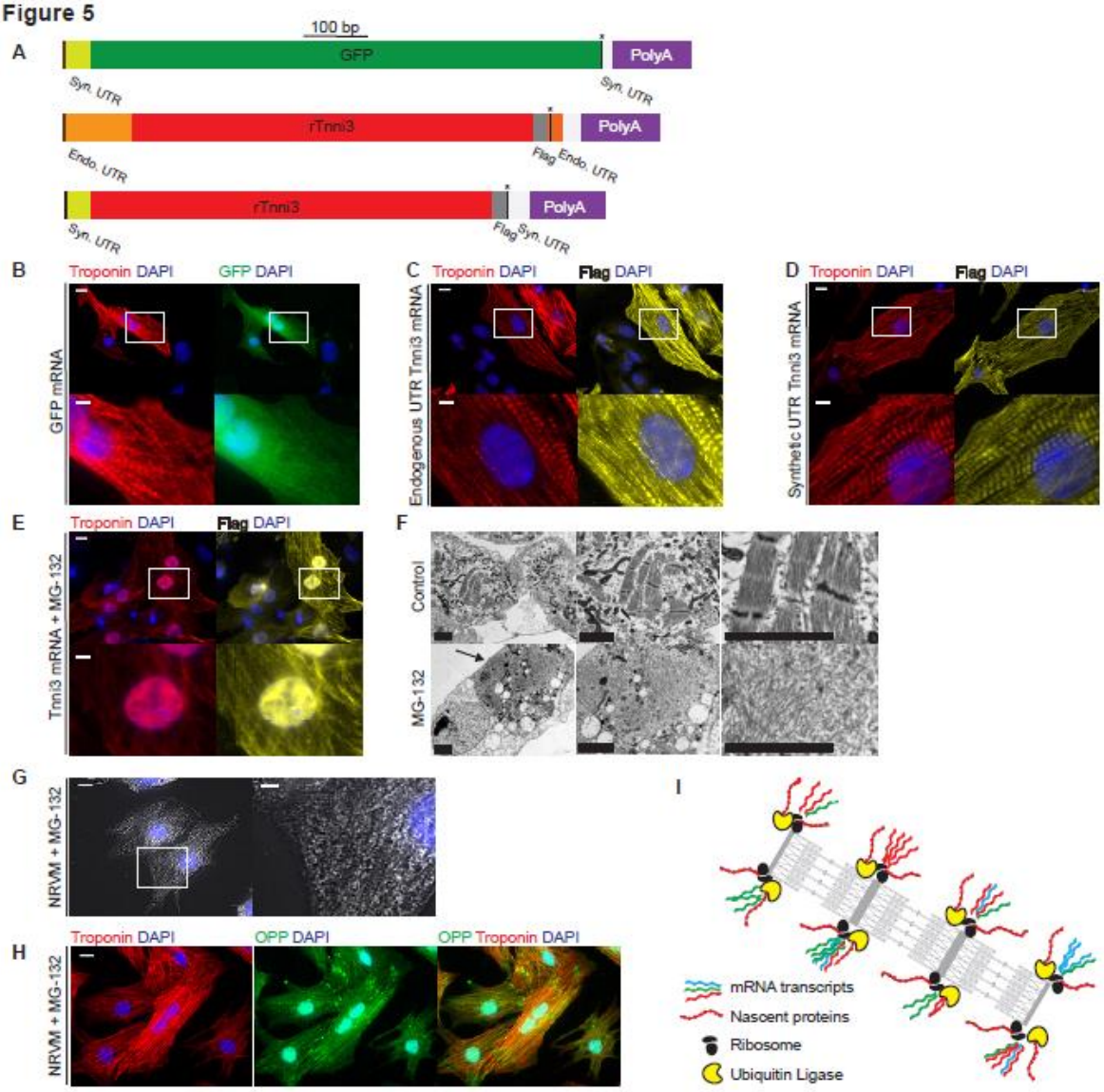

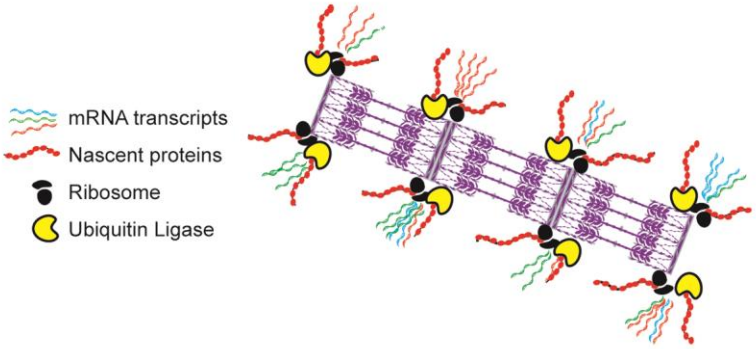

Graphical Abstract

Highlights

- The mechanisms of sarcomere maintenance in cardiomyocytes were studied
- mRNAs encoding for sarcomeric proteins are localized to the sarcomere
- Ribosomes are localized to the sarcomere with localized protein translation
- Excess sarcomeric proteins are degraded with a localized E3 ubiquitin ligase